

Title	Energy barriers at interfaces between (100) In _x Ga _{1-x} As (0 ≤ x ≤ 0.53) and atomic-layer deposited Al ₂ O ₃ and HfO ₂
Authors	Afanas'ev, V. V.;Stesmans, A.;Brammertz, G.;Delabie, A.;Sionke, S.;O'Mahony, Aileen;Povey, Ian M.;Pemble, Martyn E.;O'Connor, Éamon;Hurley, Paul K.;Newcomb, Simon B.
Publication date	2009
Original Citation	Afanas'ev, V. V., Stesmans, A., Brammertz, G., Delabie, A., Sionke, S., O'Mahony, A., Povey, I. M., Pemble, M. E., O'Connor, E., Hurley, P. K. and Newcomb, S. B. (2009) 'Energy barriers at interfaces between (100) In _x Ga _{1-x} As (0 ≤ x ≤ 0.53) and atomic-layer deposited Al ₂ O ₃ and HfO ₂ ', Applied Physics Letters, 94(20), pp. 202110. doi: 10.1063/1.3137187
Type of publication	Article (peer-reviewed)
Link to publisher's version	http://aip.scitation.org/doi/abs/10.1063/1.3137187 - 10.1063/1.3137187
Rights	© 2009 American Institute of Physics.This article may be downloaded for personal use only. Any other use requires prior permission of the author and AIP Publishing. The following article appeared in Afanas'ev, V. V., Stesmans, A., Brammertz, G., Delabie, A., Sionke, S., O'Mahony, A., Povey, I. M., Pemble, M. E., O'Connor, E., Hurley, P. K. and Newcomb, S. B. (2009) 'Energy barriers at interfaces between (100) In _x Ga _{1-x} As (0 ≤ x ≤ 0.53) and atomic-layer deposited Al ₂ O ₃ and HfO ₂ ', Applied Physics Letters, 94(20), pp. 202110 and may be found at http://aip.scitation.org/doi/abs/10.1063/1.3137187
Download date	2024-04-25 10:42:01
Item downloaded from	https://hdl.handle.net/10468/4360



University College Cork, Ireland
Coláiste na hOllscoile Corcaigh

Energy barriers at interfaces between (100) $\text{In}_x\text{Ga}_{1-x}\text{As}$ ($0 \leq x \leq 0.53$) and atomic-layer deposited Al_2O_3 and HfO_2

V. V. Afanas'ev¹, A. Stesmans, G. Brammertz, A. Delabie, S. Sionke, A. O'Mahony, I. M. Povey, M. E. Pemble, E. O'Connor, P. K. Hurley, and S. B. Newcomb

Citation: *Appl. Phys. Lett.* **94**, 202110 (2009); doi: 10.1063/1.3137187

View online: <http://dx.doi.org/10.1063/1.3137187>

View Table of Contents: <http://aip.scitation.org/toc/apl/94/20>

Published by the [American Institute of Physics](#)

Articles you may be interested in

1-nm-capacitance-equivalent-thickness $\text{HfO}_2/\text{Al}_2\text{O}_3/\text{InGaAs}$ metal-oxide-semiconductor structure with low interface trap density and low gate leakage current density

Applied Physics Letters **100**, 132906 (2012); 10.1063/1.3698095



Energy barriers at interfaces between (100) $\text{In}_x\text{Ga}_{1-x}\text{As}$ ($0 \leq x \leq 0.53$) and atomic-layer deposited Al_2O_3 and HfO_2

V. V. Afanas'ev,^{1,a)} A. Stesmans,¹ G. Brammertz,² A. Delabie,² S. Sionke,² A. O'Mahony,³ I. M. Povey,³ M. E. Pemble,³ E. O'Connor,³ P. K. Hurley,³ and S. B. Newcomb⁴

¹Department of Physics, University of Leuven, Celestijnenlaan 200D, B-3001 Leuven, Belgium

²IMEC, Kapeldreef 75, B-3001 Leuven, Belgium

³Tyndall National Institute, University College Cork, Lee Maltings, Prospect Row, Cork, Ireland

⁴Glebe Scientific Ltd., Newport, Tipperary, Ireland

(Received 26 March 2009; accepted 27 April 2009; published online 21 May 2009)

The electron energy band alignment at interfaces of $\text{In}_x\text{Ga}_{1-x}\text{As}$ ($0 \leq x \leq 0.53$) with atomic-layer deposited insulators Al_2O_3 and HfO_2 is characterized using internal photoemission and photoconductivity experiments. The energy of the $\text{In}_x\text{Ga}_{1-x}\text{As}$ valence band top is found to be only marginally influenced by the semiconductor composition. This result suggests that the known bandgap narrowing from 1.42 to 0.75 eV when the In content increases from 0 to 0.53 occurs mostly through downshift of the semiconductor conduction band bottom. It finds support from both electron and hole photoemission data. Similarly to the GaAs case, electron states originating from the interfacial oxidation of $\text{In}_x\text{Ga}_{1-x}\text{As}$ lead to reduction in the electron barrier at the semiconductor/oxide interface. © 2009 American Institute of Physics. [DOI: 10.1063/1.3137187]

The $\text{In}_x\text{Ga}_{1-x}\text{As}$ semiconducting alloys with their known superb high-frequency performance are the leading contenders to replace Si in high-speed metal-insulator-semiconductor (MIS) devices. The key requirement for the gate stack is a high barrier for electrons and holes in the semiconductor, which would need large band offsets at MIS interfaces. Yet, there is significant uncertainty regarding band offset values at the interfaces of $\text{In}_x\text{Ga}_{1-x}\text{As}$ with oxides: Over seemingly identically fabricated $\text{In}_{0.53}\text{Ga}_{0.47}\text{As}/\text{HfO}_2$ structures a variation in the valence band (VB) offset up to 0.5 eV is reported,^{1,2} which substantially exceeds the ~ 0.3 eV VB shift between GaAs and $\text{In}_{0.53}\text{Ga}_{0.47}\text{As}$ recently reported for the interface with HfO_2 .³ This uncertainty (confusion) is likely caused by the insulator charging.⁴ An additional problem is associated with incorporation of In into the “native” oxide interlayer (IL) formed when depositing the insulator, which may cause significant reduction of the interface barrier height as, for instance, is observed at interfaces of Ge and GaAs with Al_2O_3 and HfO_2 .^{5,6}

Here we report on band offsets at the interfaces between $\text{In}_x\text{Ga}_{1-x}\text{As}$ ($x \leq 0.53$) and atomic-layer deposited (ALD) Al_2O_3 and HfO_2 as measured by internal photoemission (IPE) and photoconductivity (PC) spectroscopy. The narrowing of the $\text{In}_x\text{Ga}_{1-x}\text{As}$ gap with increasing In content is found to occur mainly through a downshift of the $\text{In}_x\text{Ga}_{1-x}\text{As}$ conduction band (CB) edge while the VB top remains at the same energy within an accuracy of 0.1 eV.

Samples were prepared on $n\text{-In}_x\text{Ga}_{1-x}\text{As}$ [$n_D \sim (1-5) \times 10^{17} \text{ cm}^{-3}$] layers grown epitaxially on (100)GaAs ($x = 0, 0.15, 0.30$) or on (100)InP ($x = 0.53$). We compared 10 nm thick ALD films of Al_2O_3 [$\text{Al}(\text{CH}_3)_3 + \text{H}_2\text{O}$ precursors at 300 °C] to 10–24 nm thick HfO_2 films [$\text{HfCl}_4 + \text{H}_2\text{O}$ or $\text{Hf}[\text{N}(\text{CH}_3)_2]_4 + \text{H}_2\text{O}$ precursors at 300 or 250 °C, respectively] (in ALD the metal precursor pulse was injected first). These oxides exhibit distinctly different interface morphology when deposited on $\text{In}_{0.53}\text{Ga}_{0.47}\text{As}$. Transmission electron

microscopy (TEM) finds no IL at the $\text{In}_{0.53}\text{Ga}_{0.47}\text{As}/\text{Al}_2\text{O}_3$ interface, while a ~ 1 nm thick IL is seen in the $\text{In}_{0.53}\text{Ga}_{0.47}\text{As}/\text{HfO}_2$ samples (cf. Fig. 1). Apparently, during ALD of Al_2O_3 the residual As oxides are removed while In and Ga oxides are dissolved in alumina, as suggested by TEM images revealing a ~ 3 nm thick alumina layer with a higher density, and by the results of time-of-flight mass spectrometry (not shown) indicating the presence of an intermixed interfacial region comprised of In, Ga, and Al oxides. The band alignment at the $\text{In}_x\text{Ga}_{1-x}\text{As}$ interfaces was determined using measurements of IPE and PC at room temperature on MIS capacitors formed by evaporation of semitransparent Au or Al electrodes on the top of Al_2O_3 and HfO_2 layers. The oxide gap width and the electron and hole barrier heights are obtained from the spectral thresholds of the PC and IPE quantum yield (Y) defined in terms of photocurrent per incident photon.^{7,8}

Logarithmic plots of the yield Y are shown in Fig. 2 for MIS capacitors with 10 nm thick Al_2O_3 (a) and HfO_2 (b)

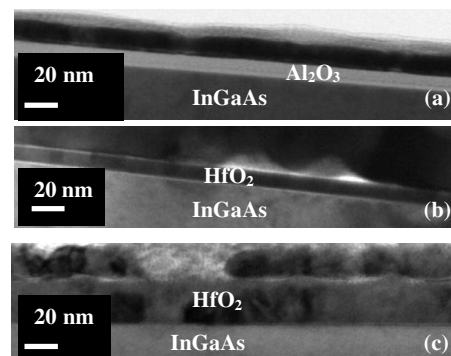


FIG. 1. TEM cross-sectional images of $\text{In}_{0.53}\text{Ga}_{0.47}\text{As}/\text{Al}_2\text{O}_3$ (a) and $\text{In}_{0.53}\text{Ga}_{0.47}\text{As}/\text{HfO}_2$ interfaces grown using two different Hf precursors HfCl_4 (b), and $\text{Hf}[\text{N}(\text{CH}_3)_2]_4$ (c), the latter resulting in a thicker, partially crystallized HfO_2 layer. Note a contrast change over the Al_2O_3 layer indicative of in-diffusion of substrate element(s) atoms, as well as the presence of a well-defined IL seen in the HfO_2 case (b) as a narrow bright band.

^{a)}Electronic mail: valeri.afanasiev@fys.kuleuven.be.

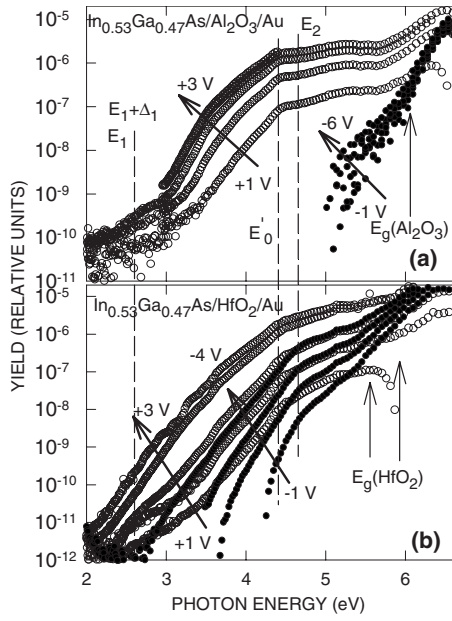


FIG. 2. Logarithmic plots of the IPE and PC spectra in $\text{In}_{0.53}\text{Ga}_{0.47}\text{As}/\text{Al}_2\text{O}_3(10 \text{ nm})/\text{Au}$ (a) and $\text{In}_{0.53}\text{Ga}_{0.47}\text{As}/\text{HfO}_2(10 \text{ nm})/\text{Au}$ (b) samples measured under positive (○: 1.0, 1.5, 2.0, 2.5, or 3.0 V), or negative (●: -1, -2, -3, -4, or -6 V) bias on the Au electrode. The vertical lines indicate energies of optical singularities in $\text{In}_{0.53}\text{Ga}_{0.47}\text{As}$; vertical arrows mark thresholds in the PC of Al_2O_3 and HfO_2 .

insulators deposited on epitaxial $\text{In}_{0.53}\text{Ga}_{0.47}\text{As}$ layers grown on InP as measured under different positive (open circles) and negative (filled circles) bias applied to the Au top electrode. In the photon energy range $h\nu < 5.5 \text{ eV}$ the dominant contribution to the photocurrent measured under positive bias stems from electron IPE from the $\text{In}_x\text{Ga}_{1-x}\text{As}$ VB to the oxide CB. This is suggested by the absence of a comparable photocurrent when the metal is biased negatively as well as by modulation of the IPE spectra⁸ at photon energies of 2.6–2.8 eV ($E_1, E_1 + \Delta_1$), 4.5 eV (E'_0) and 4.7 eV (E_2) in Fig. 2 corresponding to excitation of direct optical transitions in $\text{In}_{0.53}\text{Ga}_{0.47}\text{As}$.^{9–12} At higher photon energies the photocurrents measured under positive and negative metal bias become close and exhibit the same spectral distribution, suggesting that the signal is due to the intrinsic oxide PC. This allows one to infer the bandgap (E_g) of Al_2O_3 and HfO_2 , found to be equal to $6.1 \pm 0.1 \text{ eV}$, typical of low-temperature deposited alumina,⁷ and $5.6/5.9 \pm 0.1 \text{ eV}$, respectively (cf. arrows in Fig. 2). In the $\text{In}_{0.53}\text{Ga}_{0.47}\text{As}/\text{HfO}_2$ sample the IL-assisted electron injection becomes more pronounced with increasing positive bias resulting in an additional “low” threshold.⁶ The yield measured under negative bias in this sample is enhanced near $E_2 = 4.7 \text{ eV}$, suggesting hole IPE from the $\text{In}_{0.53}\text{Ga}_{0.47}\text{As}$ into HfO_2 and enabling determination of the barrier height between the top of the oxide VB and the bottom of CB in $\text{In}_{0.53}\text{Ga}_{0.47}\text{As}$, which is equal to $3.2 \pm 0.2 \text{ eV}$.

To monitor the energy of the $\text{In}_{0.53}\text{Ga}_{0.47}\text{As}$ VB as a function of In content, quantum yield spectra have been measured, as illustrated in Fig. 3, for MIS capacitors with Al_2O_3 (a) and HfO_2 (b) insulators deposited on $\text{In}_x\text{Ga}_{1-x}\text{As}$ with different In concentration. The curves shown are measured under positive bias corresponding to an average strength of the electric field in the oxide (F) of 2 and 1.5 MV/cm for the Al_2O_3 and HfO_2 insulators, respectively. The important find-

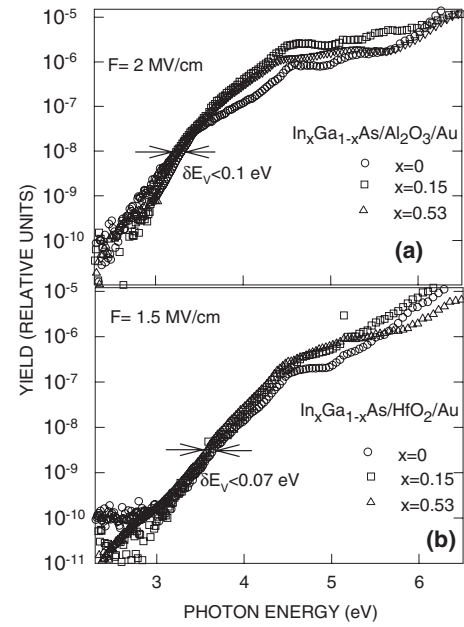


FIG. 3. Logarithmic plots of the IPE and PC yield spectra in samples with Al_2O_3 (a) and HfO_2 (b) insulators on $\text{In}_x\text{Ga}_{1-x}\text{As}$ for different In fraction in the semiconductor, measured under positive bias applied to the top metal electrode at values corresponding to the indicated strength of electric field in the oxide. Arrows show the upper limit of the semiconductor VB shift (ΔE_V) with changing x .

ing here is that the increase in the In fraction from 0 to 0.53 does not lead to any substantial spectral shift in the IPE curves within the error margins (0.07–0.1 eV) indicated by arrows. In the case of Al_2O_3 [Fig. 3(a)], the yield of direct electron IPE into the alumina CB ($3.5 < h\nu < 5.5 \text{ eV}$) becomes higher in the In-containing samples compared to the pure GaAs, which is consistent with “dissolution” of the “native” oxide IL in Al_2O_3 as revealed by TEM. Nevertheless, the IL-assisted IPE is not completely eliminated.

Spectral thresholds of electron and hole IPE were obtained from $Y^{1/3}-h\nu$ and $Y^{1/2}-h\nu$ plots, respectively,⁸ as exemplified for an $\text{In}_x\text{Ga}_{1-x}\text{As}/\text{Al}_2\text{O}_3$ sample in Fig. 4 by $Y^{1/3}-h\nu$ plots measured under incrementally enhanced positive metal bias. The plots reveal two contributions to the electron IPE; The direct IPE from the VB of $\text{In}_x\text{Ga}_{1-x}\text{As}$ into

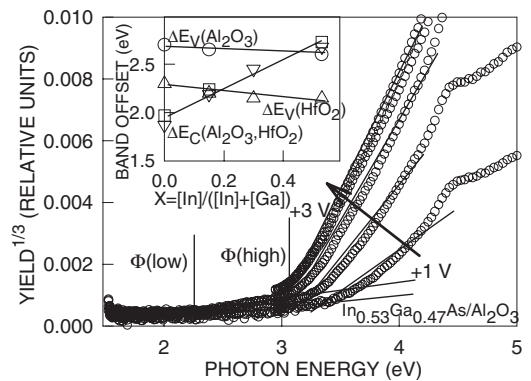


FIG. 4. Cube root of the IPE quantum yield as a function of photon energy as measured in $\text{In}_x\text{Ga}_{1-x}\text{As}/\text{Al}_2\text{O}_3(10 \text{ nm})/\text{Au}$ MIS capacitors under positive bias on the metal electrode increasing from 1 to 3 V in 0.5 V steps. Vertical lines mark two resolved spectral thresholds, $\Phi(\text{high})$ and $\Phi(\text{low})$, corresponding to the direct electron IPE to alumina CB and the IL-assisted transitions, respectively. The inset shows the CB and VB offsets at the interfaces of $\text{In}_x\text{Ga}_{1-x}\text{As}$ with Al_2O_3 and HfO_2 as a function of In content x .

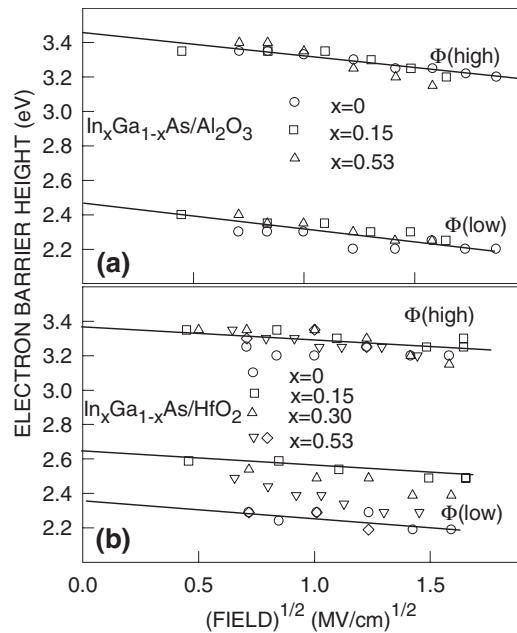


FIG. 5. Schottky plots of the electron IPE spectral thresholds in $\text{In}_x\text{Ga}_{1-x}\text{As}/\text{Al}_2\text{O}_3$ (a) and $\text{In}_x\text{Ga}_{1-x}\text{As}/\text{HfO}_2$ (b) samples with different content x of In in the semiconductor. The “high” threshold corresponds to the energy barrier between the top of the $\text{In}_x\text{Ga}_{1-x}\text{As}$ VB and the bottom of the oxide CB. The “low” barrier stems from the electron IPE mediated by the narrow-gap $\text{In}_x\text{Ga}_{1-x}\text{As}$ “native” oxide present at the interface.

the oxide CB characterized by the “high” IPE threshold [$\Phi(\text{high})$] and the IL-assisted IPE with the “low” [$\Phi(\text{low})$] barrier.⁸ Values of these barriers measured in samples with different In content are shown in Figs. 5(a) and 5(b) as functions of applied electric field. These Schottky plots were used to determine the zero-field barrier height corresponding to the band offset at the $\text{In}_x\text{Ga}_{1-x}\text{As}/\text{oxide}$ interface (unaffected by the image-force effect). In the Al_2O_3 -samples the barriers for both direct IPE into the oxide CB and for the IL-mediated transitions are insensitive to the In content within an accuracy of 0.1 eV, importantly indicating that (a) the energy of the semiconductor VB top remains fixed at 3.45 ± 0.10 eV below the alumina CB bottom and, (b) the possible presence of In in the near-interfacial oxide does not lead to additional barrier lowering.

In the case of HfO_2 the barrier between the top of the $\text{In}_x\text{Ga}_{1-x}\text{As}$ VB and the bottom of the oxide CB is 3.35 ± 0.10 eV and, like in the case of Al_2O_3 , shows little sensitivity to the In content. Consistent with this result, the hole IPE threshold at the $\text{In}_x\text{Ga}_{1-x}\text{As}/\text{HfO}_2$ interface is found at 3.2 ± 0.2 eV as compared to 3.8 ± 0.2 eV in GaAs/HfO_2 , indicating a downshift of the semiconductor CB bottom with increasing In content. By contrast, the observed spread in the low spectral threshold values corresponding to the IL-assisted electron IPE into HfO_2 may be caused by the different thickness of the IL and/or its composition. This is suggested by differences in the $\Phi(\text{low})$ values observed in samples with HfO_2 layers deposited from different Hf precursors [cf. symbols ∇ and \diamond in Fig. 5(b) corresponding to ALD from $\text{HfCl}_4 + \text{H}_2\text{O}$ and $\text{Hf}[\text{N}(\text{CH}_3)_2]_4 + \text{H}_2\text{O}$, respectively]. Changes in the IL-related barrier would also explain the earlier reported sensitivity of IPE in $\text{GaAs}/\text{Al}_2\text{O}_3$ entities to the semiconductor surface preparation.¹³ At the same time,

the barrier $\Phi(\text{high})$, corresponding to direct electron IPE into the oxide CB, appears to be insensitive to the HfO_2 deposition process [cf. Fig. 5(a)] affirming its fundamental character.

As a final step, the fundamental CB (ΔE_C) and VB (ΔE_V) offsets at the interfaces of $\text{In}_x\text{Ga}_{1-x}\text{As}$ with Al_2O_3 and HfO_2 were calculated from the measured barrier between the semiconductor VB and the oxide CB, combined with the oxide bandgap width. We have found that the top of the $\text{In}_x\text{Ga}_{1-x}\text{As}$ VB remains at the same energy below the Al_2O_3 CB (3.45 ± 0.10 eV) and HfO_2 CB (3.35 ± 0.10 eV) when the In content x increases from 0 to 0.53. This corresponds to a CB offset increase from approximately 2 eV for GaAs to 2.7 eV for $\text{In}_{0.53}\text{Ga}_{0.47}\text{As}$ (cf. inset in Fig. 4), promising an improvement in the gate insulation. This result is consistent with the band offsets observed in strained $\text{GaAs}/\text{In}_x\text{Ga}_{1-x}\text{As}$ quantum well structures where the CB offset accounts for 85% of the bandgap difference.¹⁴ Calculations based on the charge neutrality concept also suggest that the VBs of GaAs and InAs are aligned at their interfaces with HfO_2 (the “common anion” case),¹⁵ making it also unlikely that the VB top energy would vary at the interfaces of $\text{In}_x\text{Ga}_{1-x}\text{As}$ with the same oxide. Like at the interfaces of GaAs with the currently studied oxides,⁶ the oxide IL formed during the ALD process provides a lower electron barrier, but this barrier reduction is insensitive to the In content in the semiconductor, suggesting that the narrow-gap In_2O_3 phase is not formed during ALD.

The work done at KU Leuven was supported by the Fonds Wetenschappelijk Onderzoek (FWO) Vlaanderen (Grant No. 1.5.057.07). The authors from the Tyndall National Institute would like to acknowledge the Science Foundation Ireland (Grant No. 07/SRC/I1172) for financial support.

¹Y. C. Chang, M. L. Huang, K. Y. Lee, Y. J. Lee, T. D. Lin, M. Hong, J. Kwo, T. S. Lay, C. C. Liao, and K. Y. Cheng, *Appl. Phys. Lett.* **92**, 072901 (2008).

²M. Kobayashi, P. T. Chen, Y. Sun, N. Goel, P. Majhi, M. Garner, W. Tsai, P. Pianetta, and Y. Nishi, *Appl. Phys. Lett.* **93**, 182103 (2008).

³M. L. Huang, Y. C. Chang, Y. H. Chang, T. D. Lin, J. Kwo, and M. Hong, *Appl. Phys. Lett.* **94**, 052106 (2009).

⁴See, e.g., W. M. Lau, *Appl. Phys. Lett.* **54**, 338 (1989); *J. Appl. Phys.* **67**, 1504 (1990).

⁵V. V. Afanas'ev, A. Stesmans, A. Delabie, F. Bellenger, M. Houssa, and M. Meuris, *Appl. Phys. Lett.* **92**, 022109 (2008).

⁶V. V. Afanas'ev, M. Badylevich, A. Stesmans, G. Brammertz, A. Delabie, S. Sionke, A. O'Mahony, I. M. Povey, M. E. Pemble, E. O'Connor, P. K. Hurley, and S. B. Newcomb, *Appl. Phys. Lett.* **93**, 212104 (2008).

⁷V. V. Afanas'ev and A. Stesmans, *J. Appl. Phys.* **102**, 081301 (2007).

⁸V. V. Afanas'ev, *Internal Photoemission Spectroscopy: Principles and Applications* (Elsevier, Amsterdam, 2008).

⁹E. H. Perea, E. M. Mendez, and C. G. Fonstad, *Appl. Phys. Lett.* **36**, 978 (1980).

¹⁰D. E. Aspnes and H. J. Stocker, *J. Vac. Sci. Technol.* **21**, 413 (1982).

¹¹V. I. Gavrilenko, A. M. Grekhov, D. V. Korbutyak, and V. G. Litovchenko, *Optical Properties of Semiconductors* (Naukova Dumka, Kiev, 1987).

¹²T. W. Nee and A. K. Green, *J. Appl. Phys.* **68**, 5314 (1990).

¹³N. V. Nguyen, O. A. Kirillov, W. Jia, W. Wang, J. S. Suehle, P. D. Ye, Y. Xuan, N. Goel, K.-W. Choi, W. Tsai, and S. Sayan, *Appl. Phys. Lett.* **93**, 082105 (2008).

¹⁴D. J. Arent, K. Deneffe, C. Van Hoof, J. De Boek, and G. Borghs, *J. Appl. Phys.* **66**, 1739 (1989).

¹⁵J. Robertson and B. Falabretti, *J. Appl. Phys.* **100**, 014111 (2006).